BMC Microbiology

RESEARCH Open Access

Ornithinibacillus liuyingii sp. nov.: a novel multidrug-resistant and potentially pathogenic bacterium isolated from *Apodemus chevrieri* lung tissue

Jian Zhou[1,2†], Tao Gu[1,2†], Ya Zhang[3], Jingzhu Zhou[2], Xiaoxiao Zeng[1,2], Fengming Chen[2], Yong Hu[1*] and Shijun Li[1,2*]

Abstract

Ornithinibacillus liuyingii sp. nov. was proposed, with type strain 27F3^T (=GDMCC 1.5626^T=JCM 38003^T) isolated from the lung of *Apodemus chevrieri* collected on the Guizhou Plateau, China. Phylogenetic distinctiveness from its closest relative, *Ornithinibacillus scapharcae* TW25^T, was confirmed by 98.5% 16S rRNA gene similarity, 76.98% average nucleotide identity, and 21.9% digital DNA–DNA hybridization value. Phenotypically, strain 27F3^T was characterized as a motile, rod-shaped bacterium exhibiting a Gram-stain-negative reaction, an atypical feature within the otherwise Gram-positive genus *Ornithinibacillus*. The strain formed greyish-light purple colonies and displayed a distinct antimicrobial resistance profile, including resistance to cefepime, polymyxin E, and nalidixic acid. Chemotaxonomic analysis revealed iso-$C_{15:0}$, anteiso-$C_{15:0}$, and iso-$C_{17:0}$ as major fatty acids and menaquinone MK-7 as the predominant respiratory quinone. Genomic analysis identified genes associated with sporulation and oxidative stress defense, and numerous homologs of virulence-associated factors were detected. However, 16S rRNA gene amplicon sequencing of 90 additional rodent lungs did not detect close relatives (max identity 95.8%), suggesting that *O. liuyingii* should not be a common colonizer. This study describes the *Ornithinibacillus* species isolated from a mammalian respiratory tract and highlights its atypical Gram-stain reaction, which may contributing to our understanding into the diversity of the genus. The discovery may underscore the hidden complexity within wildlife-associated microbiota and emphasizes the importance of pathogen surveillance in a One Health context.

Keywords *Ornithinibacillus liuyingii* sp. nov., Phylogenetic analysis, Polyphasic taxonomy, Whole-genome sequencing, Genomic function, 16S rRNA gene sequence

†Jian Zhou and Tao Gu are joint first authors who contributed equally to this work.

*Correspondence:
Yong Hu
huyong1979@gmc.edu.cn
Shijun Li
zjumedjun@163.com

[1]The Key Laboratory of Environmental Pollution Monitoring and Disease Control, Ministry of Education, School of Public Health, Guizhou Medical University, Guiyang 550025, China
[2]Key Laboratory of Microbio and Infectious Disease Prevention and Control in Guizhou Province, Guizhou Center for Disease Control and Prevention, Guiyang 550004, China
[3]School of Basic Medicine, Guizhou University of Traditional Chinese Medicine, Guiyang 550025, China

Background

The microbial world harbours vast, unexplored diversity with significant implications for understanding evolution, ecology, and host–microbe interactions. Within the order *Bacillales* of the phylum *Bacillota*, the genus *Ornithinibacillus*—currently comprising 10 validly published species (LPSN 2025)—serves as a model for studying microbial adaptation to extreme conditions. Members of this genus have been isolated from a range of habitats, including deep-sea sediments (*O. californiensis*) [1], saline soils (*O. salinisoli*) [2], and dairy products (*O. bavariensis*) [1], often exhibiting traits such as alkaline protease production and stress-tolerance mechanisms. Despite this ecological breadth, *Ornithinibacillus* species has not been reported in association with mammalian hosts, representing a gap in understanding their potential role in host–associated microbiomes.

Small mammals inhabiting high-altitude ecosystems may provide valuable insights into microbial adaptation to hypoxic and low-temperature stress. The respiratory microbiota of *Apodemus chevrieri*—the dominant rodent species across the Yunnan-Guizhou Plateau in China (1,500–3,000 m above sea level)—remains poorly characterised, yet may offer clues to host–microbe coevolution under environmental constraints [3, 4]. Wildlife-associated microbes harbored by such hosts may encode distinctive adaptive traits, serving as models for ecological research [5].

To address this knowledge gap, we isolated strain 27F3^T from lung tissue of *A. chevrieri* collected in Weining County, Guizhou Province, at an altitude of 2,248 m. A polyphasic taxonomic approach confirmed its novelty based on 16S rRNA gene sequence divergence (< 98.7% similarity), whole-genome relatedness indices (ANI < 95%; dDDH < 70%) [6], and functional genomic features potentially associated with adaptation to the respiratory microenvironment. This study may extend the known ecological range of the genus *Ornithinibacillus* to include vertebrate hosts, offers a framework for investigating high-altitude host–microbe interactions, and revealed genomic traits relevant to antibiotic resistance and immunomodulation research.

Materials and methods

Source of animals and anesthesia

The bacterial strain described in this study was isolated during a systematic survey investigating the respiratory microbiota of small mammals inhabiting the high-altitude regions of Guizhou Plateau. This ecological investigation aimed to identify host-associated bacteria that may exhibit unique adaptations to hypoxic and low-temperature environments. *A. chevrieri* was specifically selected as the target species because it is the dominant rodent within this ecosystem (at elevations of 1,500–3,000 m) and serves as a key sentinel species for studying environmental and microbial adaptation. Wild *A. chevrieri* individuals weighing less than 200 g were captured in their natural habitat using live traps. Following capture, the animals were housed and managed by the Guizhou Provincial Center for Disease Control and Prevention. Prior to euthanasia, the mice were anesthetized via intraperitoneal injection of sodium pentobarbital (3% concentration, 50 mg/kg). Humane euthanasia was subsequently performed by trained personnel through cervical dislocation while the animals were under deep anesthesia. All anesthetic and euthanasia procedures adhered to the guidelines issued by the American Veterinary Medical Association (AVMA) and complied with Chinese regulations on laboratory animal welfare to minimize distress and suffering.

Isolation and cultivation of bacterial strains

Lung tissue samples were aseptically collected from wild *A. chevrieri* in Weining County, Guizhou Province (26°36' N, 104°16' E; Elevation 2,248 m). All dissections were carried out in a specialized and clean laboratory environment at the disease control center where the sampling site is located. Prior to dissection, the external surface of the euthanized animals was thoroughly disinfected with 70% ethanol to minimize surface contamination. All surgical instruments (surgical knives, forceps, scissors) were sterilized by autoclaving (121 °C, 20 min) and used only once for each animal, or sterilized again between each operation. Aseptic operation was maintained throughout the procedure. To access the lung tissue, a sterile ventral midline incision was made following skin disinfection. The thoracic cavity was opened using sterile instruments, exposing the lungs. A section of peripheral lung tissue (approximately 0.5 cm^3) was aseptically excised using sterile surgical tools, taking care to avoid cross-contamination from the gastrointestinal tract or skin. The excised tissue sample was immediately placed into a sterile test tube containing pre-sterilized brain heart infusion (BHI) culture medium. The tube was sealed, stored in dry ice, and transported to our laboratory within 4 h. Upon arrival, the sample was processed immediately for bacterial isolation. Tissue homogenates were vortexed thoroughly, and 100 µL aliquots were plated onto Columbia blood agar supplemented with 5% defibrinated sheep blood. Plates were incubated at 37 °C in a 5% CO_2 atmosphere for 48 h. Morphologically distinct colonies were purified through two successive subcultures.

16S rRNA gene amplification and phylogenetic reconstruction

Bacterial genomic DNA was extracted with the Baiyi Bacterial DNA Extraction Kit (Hangzhou Baiyi Technology). The nearly full-length 16S rRNA gene was amplified with

primers 27 F (5′-AGAGTTTGATCMTGGCTCAG-3′) and 1492R (5′-TACGGYTACCTTGTTACGACTT-3′). Each 50 μL PCR mixture contained 25 μL of Premix Taq (Takara), 2 μL of each primer (10 μM), approximately 50 ng of genomic DNA template, and ddH_2O to a final volume of 50 μL. Thermal cycling conditions were as follows: initial denaturation at 94 °C for 10 min; 30 cycles of 94 °C for 30 s, 52 °C for 30 s, and 72 °C for 60 s; and final extension at 72 °C for 10 min. PCR Products were purified and t subsequently sequenced by Tsingke Biotechnology.

The resulting 16S rRNA gene sequence was compared against those of type strains available in the NCBI database using BLASTn. Sequences exhibiting < 98.7% similarity were considered putatively novel [7]. All validly published 16S rRNA gene sequences of the genus Ornithinibacillus were retrieved from the List of Prokaryotic names with Standing in Nomenclature (LPSN, https://lpsn.dsmz.de/) and aligned using Clustal_W implemented in MEGA11 [7]. The resulting multiple sequence alignment was manually inspected and trimmed at both ends to ensure all sequences spanned the same homologous region. The final alignment used for phylogenetic reconstruction contained 1,350 nucleotide positions. Phylogenetic trees were inferred using Neighbor-Joining (NJ) [8] and Maximum-Likelihood (ML) [9] methods with bootstrap values calculated from 1,000 replicates.

Whole-genome sequencing and assembly

The whole genome of the strain was sequenced on the Illumina NovaSeq X Plus platform. Genomic DNA was extracted with the DNeasy PowerSoil Pro Kit (Qiagen) following enzymatic treatment with lysozyme (10 mg/mL, Sigma-Aldrich) at 37 °C for 30 min. DNA quality and concentration were determined using a Nanodrop 2000 spectrophotometer (Thermo Fisher Scientific) and a Qubit 4.0 Fluorometer (Invitrogen). Genomic DNA was fragmented to approximately 350 bp using a Covaris LE220 sonicator (10% duty factor, 200 cycles per burst, 90 s duration). Library construction involved end repair, adenylation, and adapter ligation with unique dual-indexed Illumina adapters (IDT for Illumina DNA/RNA UD Indexes). Libraries were amplified with six cycles of PCR using KAPA HiFi HotStart ReadyMix (Roche) under the following program: 98 °C for 45 s; 6 cycles of 98 °C for 15 s, 60 °C for 30 s, and 72 °C for 30 s; final extension at 72 °C for 5 min. Fragment size distribution was evaluated on an Agilent 4200 TapeStation with D1000 ScreenTape. Sequencing was performed in 2 × 150 bp paired-end mode with 20% PhiX control to compensate for low sequence diversity. Base calling and real-time quality monitoring were conducted using the DRAGEN Bio-IT Platform v4.2 (Illumina), achieving Q30 scores above 85%.

Bioinformatic processing included raw read quality control with FastQC v0.12.1 [10], adapter trimming and quality filtering via Trimmomatic v0.39 (parameters: SLIDINGWINDOW:4:20, MINLEN:100) [11], de novo hybrid assembly using SPAdes v3.15.5 (k-mer sizes 21–127) [12], and three iterative rounds of error correction with Pilon v1.24 based on at least 100× coverage data [13], and the completeness and contamination of the assembled genome were assessed using CheckM v1.2.2 [14].

Genomic taxonomy and phylogenomic analysis

The presence of plasmids in the genome assembly of strain $27F3^T$ was assessed using Platon v1.6 [15], a tool specifically designed for the prediction of plasmid-borne contigs in prokaryotic draft genomes. The analysis was performed in 'accuracy' mode with the default database. Contigs shorter than 500 bp were filtered out, and the remaining contigs were evaluated based on a plasmid prediction score (RDS) and the presence of hallmark genomic features, including replication initiator (*rep*) genes, mobilization (*mob*) genes, conjugation systems, antimicrobial resistance (AMR) genes, rRNA operons, and sequence similarity to known plasmid references. CRISPR arrays were identified using CRISPR-CasFinder [16], and prophage regions were predicted with PHASTER [17]. Whole-genome-sequence-based taxonomic classification was performed using GTDB-Tk v2.3.2 under the "classify" workflow with reference to the GTDB r214 database [18]. A concatenated alignment of 120 bacterial marker proteins was constructed with hmmalign and trimmed to 5,035 informative amino acid sites. To reconstruct the core-genome phylogeny, reference type strains closely related to the isolate were first identified via 16S rRNA gene sequence similarity. Their genomes were downloaded from the NCBI database and annotated with Prokka to generate GFF files [19]. The UBCG program was used to extract 92 core genes from the genomes of 11 tested strains and to perform phylogenetic tree analysis [20]. Gene prediction was subsequently conducted using Prodigal (v2.6.3), while homologous sequences were screened using HMMER (v3.3.2) [21]. The protein sequences of the core genes were aligned using MAFFT (v7), and the maximum likelihood phylogenetic trees were reconstructed using RAxML (v8.2.13) and FastTree (v2.1.10) [22], respectively.

Average nucleotide identity (ANI) was computed with FastANI v1.32 [23] and the EzBioCloud ANI calculator (www.ezbiocloud.net/tools/ani), using a species threshold of 95–96%. Digital DNA–DNA hybridization (dDDH) values were estimated via the Genome-to-Genome Distance Calculator (GGDC) v3.0 (https://ggdc.dsmz.de/ggdc.php#), with 70% similarity serving as the species delineation cutoff. All currently accepted species

and subspecies within the relevant genus were compiled from the List of Prokaryotic names with Standing in Nomenclature (LPSN; https://lpsn.dsmz.de) to ensure a comprehensive taxonomic framework. Average Amino acid Identity (AAI) was determined based on the annotated protein sequences (.faa files) generated by Prokka. An all-against-all BLASTP was performed, and the top hit for each protein was selected by sorting matches by bit score and retaining unique pairs using the Sort and Unique utilities. The mean identity of these top matches was computed as the AAI using the Summary Statistics tool (https://usegalaxy.org/tool_id=Summary_Statistics1&version=latest). This procedure was repeated across all genome pairs to generate a comprehensive AAI matrix.

Phenotypic characterization

Cell morphology was examined using transmission electron microscopy (TEM, JEM-1400FLASH, JEOL) and scanning electron microscopy (SEM, JSM-IT700HR, JEOL). Metabolic profiles were determined with Biolog GEN III MicroPlates [24]. Carbohydrate fermentation patterns were assessed using API 50CHB test strips (bioMérieux) [25], and enzymatic activities were evaluated with the API ZYM system [26]. The API 20NE kit was employed for biochemical profiling of non-enteric Gram-negative bacteria. The Gram reaction was evaluated by conventional Gram staining supplemented with the 3% KOH string test. Motility was tested by stab inoculation into semi-solid agar medium, followed by incubation at a suitable temperature and examination of growth diffusion away from the inoculation line [27]. To further assess the Gram reaction, which yielded an atypical result for the genus, Gram staining was performed in triplicate on bacterial cultures harvested at different growth phases (early-log, mid-log, and stationary phase). The 3% KOH string test was similarly repeated. In addition, the presence of genes potentially associated with the synthesis of lipopolysaccharide (LPS) or outer membrane proteins was investigated in the genome.

Chemotaxonomic profiling

Cellular fatty acids, respiratory quinones, and polar lipids were analyzed from cells cultured aerobically on Tryptic Soy Agar at 28 °C for 24 h. Fatty acid methyl esters (FAMEs) were obtained and separated by gas chromatography (Agilent 6890) using the MIDI Sherlock Microbial Identification System with the TSBA6 database [28]. Polar lipids were resolved by two-dimensional thin-layer chromatography (2D-TLC) and visualized with specific detection reagents: molybdenum blue for phospholipids, ninhydrin for aminolipids, anisaldehyde for glycolipids, and phosphomolybdic acid for total lipids [29]. Respiratory quinones were extracted using the Bligh–Dyer method and analyzed by high-performance liquid chromatography (HPLC; Agilent 1260 Infinity II) on a reversed-phase C18 column with an isopropanol–hexane (2:1, v/v) mobile phase at a flow rate of 1.0 mL/min [30].

Functional annotation of the genome

The assembled genome was functionally annotated using a multi-database approach to characterize gene functions and potential biological features. Metabolic pathway reconstruction was carried out based on the Kyoto Encyclopedia of Genes and Genomes (KEGG) [31]. Protein-coding sequences were classified into functional categories using the Clusters of Orthologous Groups (COG) database [32]. Sequence similarity searches were performed against the NCBI Non-Redundant (NR) protein database [33]. Genes potentially involved in pathogen-host interactions were screened with the Pathogen–Host Interactions database (PHI, v4.16) [34], and virulence-related factors were annotated using the Virulence Factor Database (VFDB) [35]. Gene function prediction was performed using DIAMOND against the VFDB with the following thresholds: E-value ≤ $1e^{-5}$, identity ≥ 40%, query coverage ≥ 40%, and subject coverage ≥ 40%. Only the best hit per gene was retained (max-hsps 1, –k 1).

Antimicrobial susceptibility testing

The antimicrobial susceptibility of the isolate was determined using the broth microdilution method to measure minimum inhibitory concentrations (MICs) with a custom-designed panel comprising 29 antibiotics, including β-lactams, tetracyclines, fluoroquinolones, aminoglycosides, macrolides, phenicols, polymyxins, and folate pathway antagonists. Testing was performed in cation-adjusted Mueller–Hinton broth in accordance with the standards and interpretative criteria established by the Clinical and Laboratory Standards Institute (CLSI) [36]. Susceptibility profiles (MIC values) were interpreted using the CLSI breakpoints applicable to aerobic Gram-stain-positive bacteria, as no specific criteria exist for the genus *Ornithinibacillus*. *Escherichia coli* ATCC 25,922 was included as a quality control strain to ensure accuracy and reproducibility of the results.

16S rRNA gene amplicon sequencing analysis

To investigate the prevalence of the novel bacterial species in host organisms, we performed 16S rRNA gene amplicon sequencing on lung tissues collected from rodent samples captured during the same period. A total of 90 rodents were captured in Weining County, comprising 30 individuals each of *A. chevrieri*, *Rattus losea*, and *Niviventer confucianus*. Lung tissues from three individuals of the same species were pooled into one sample for 16S rRNA gene amplicon sequencing, resulting in a total of 30 sequencing samples (10 per species: group ACL, RLL, NCL; Supplementary Table 1). Genomic DNA was

extracted using the CTAB method. The V3–V4 region of the 16S rRNA gene was amplified with primers 341 F (5′-CCTAYGGGRBGCASCAG-3′) and 806R (5′-GGACTACNNGGGTATCTAAT-3′). Libraries were constructed using the NEB Next Ultra DNA Library Prep Kit (Illumina) and sequenced on an Illumina platform (250-bp paired-end reads). Raw sequences were processed with Trimmomatic (v0.35; sliding window, quality score < 20, length < 50 bp). Paired-end reads were merged using FLASH and denoised with DADA2 in QIIME2 (v2022.2) to generate amplicon sequence variants (ASVs) [37]. Taxonomic classification was performed using the Greengenes2 database (v2022.10) [38], from which a FASTA file containing all representative 16S rRNA gene sequences (V3–V4 region) was obtained. The V3–V4 region of the novel bacterial strain was extracted and compared against the collective 16S rRNA gene sequences derived from the lung microbiota of the three rodent species via NCBI BLASTn, to determine the prevalence of this novel species within the host populations.

Results

Cultural and morphological characteristics

Strain 27F3^T was cultured on Columbia blood agar at 28 °C and 37 °C under 5% CO_2 for 48 h. Growth was negligible under anaerobic conditions. Under aerobic conditions, optimal growth occurred at 30 °C with 5% CO_2, with slower growth under other aerobic conditions. Colonies appeared smooth, moist, circular with entire margins, displaying three concentric rings: a gray-white outer ring, a pale purple middle ring, and a gray-white center ring. The strain showed gamma-hemolysis (no hemolysis) on sheep blood agar (Fig. 1A). Gram staining revealed Gram-negative rods, approximately 1–2 μm in length (Fig. 1B). The Gram-negative reaction was confirmed by both traditional staining and the 3% KOH string test, the latter of which produced a distinct viscous string. Under SEM, strain 27F3^T exhibited a rod-shaped morphology with predominantly rounded or blunt ends (Fig. 1C). Repeated Gram staining and the 3% KOH string test consistently yielded results indicative of a Gram-negative reaction across all growth phases tested. However, TEM revealed a cell envelope structure with features more commonly associated with Gram-positive bacteria, including a relatively thick, electron-dense cell wall and the absence of a visible outer membrane (Fig. 1D). Genomic analysis did not identify hallmark gene clusters for the synthesis of lipopolysaccharide (LPS), a key component of the outer membrane in canonical diderm (Gram-negative) bacteria. This discrepancy between the phenotypic staining results and the ultrastructural/genomic evidence warrants careful consideration.

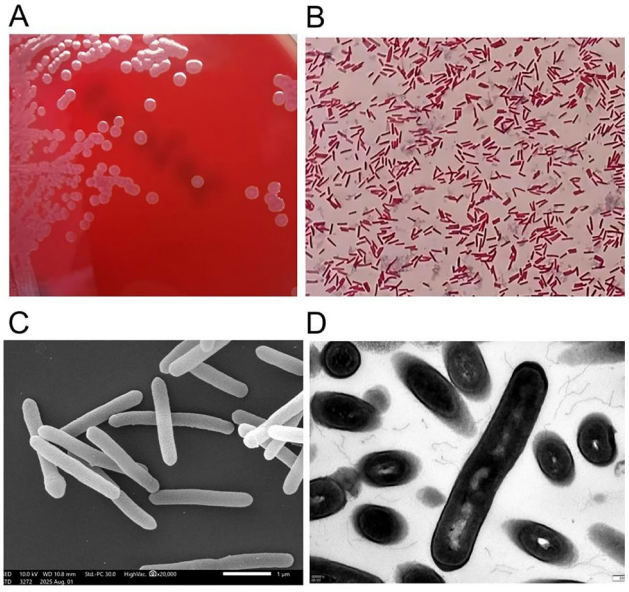

Fig. 1 Morphological characteristics of strain 27F3^T. **A** Colony morphology on Columbia blood agar after 48-h incubation. **B** Gram-stain under light microscopy (×100 oil immersion). **C** Scanning electron micrograph. **D** Transmission electron micrograph

16S rRNA gene phylogenetic analysis

The amplified and assembled 16S rRNA gene consensus sequence was 1,431 bp in length. All 16S rRNA gene sequences of the 10 validly published *Ornithinibacillus* species sequences were retrieved from the LPSN. Phylogenetic analysis showed that strain 27F3^T shared the highest similarity with *Ornithinibacillus scapharcae* TW25^T (98.5%), followed by *Ornithinibacillus bavariensis* WSBC 24,001^T (98.0%) and *Ornithinibacillus californiensis* MB-9^T (97.7%). The NJ tree placed strain 27F3^T closest to *O. scapharcae* TW25^T, then *O. californiensis* MB-9^T (Fig. 2A). The ML tree yielded a consistent topology (Fig. 2B). The 16S rRNA sequence extracted from the whole genome (1,550 bp) showed 99.9% identity with the PCR-amplified sequence when compared using NCBI BLASTn.

Notably, the 16S rRNA gene sequence of strain 27F3^T exhibited 99.8% similarity (100% coverage) to that of a strain labeled "*Ornithinibacillus massiliensis*" on the LPSN, which is indicated with the status "not validly published" (full-length 1,484 bp, NCBI accession: NR_179601). Further investigation revealed that this not-validly-named *Ornithinibacillus* strain was isolated from the fecal sample of a malnourished child in African [39].

Phylogenetic analysis based on core-genes

Phylogenetic reconstruction based on whole-genome sequences clearly delineated the position of strain 27F3^T among its closest relatives (Fig. 3). The ML tree revealed that strain 27F3^T forms a distinct and robust monophyletic clade, supported by a bootstrap value of 86%, confirming its status as a separate species within the genus

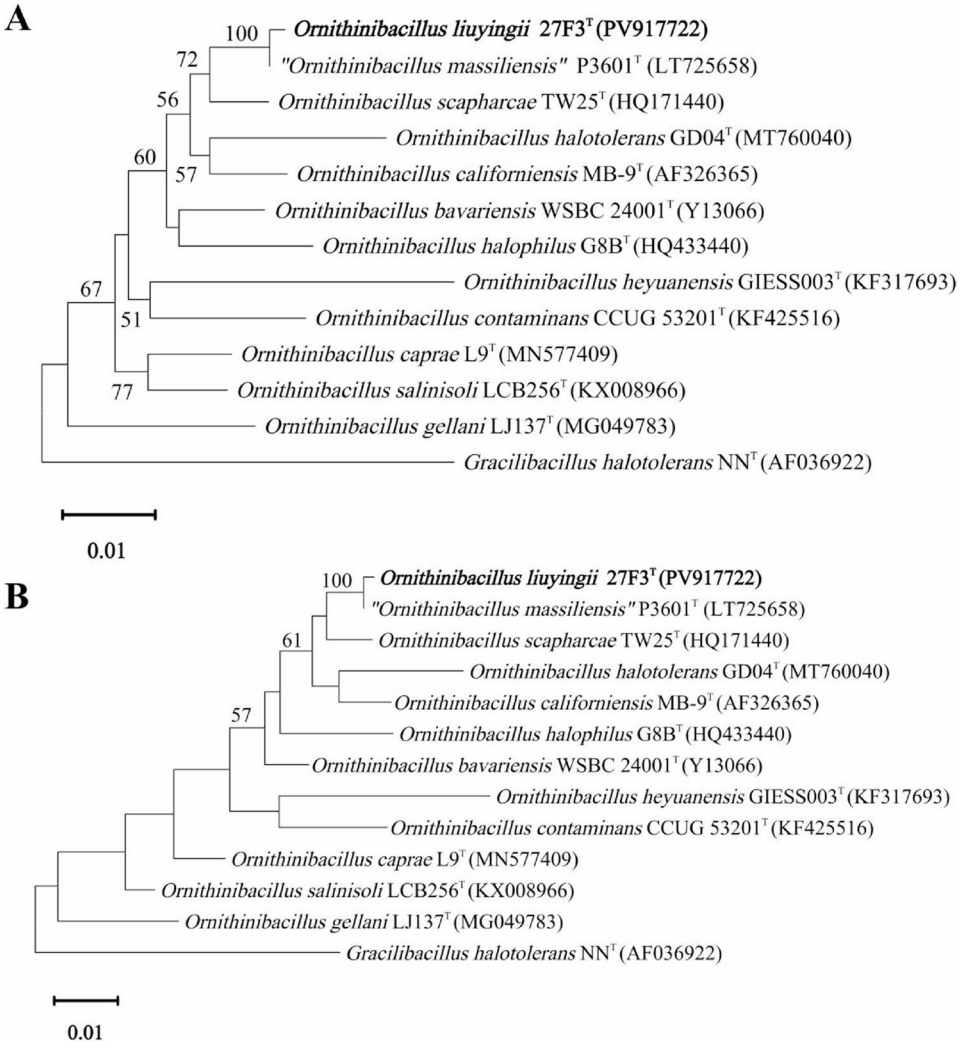

Fig. 2 Phylogenetic analysis based on 16S rRNA gene sequences of strain27F3^T and related taxa. **A** Neighbor-joining (NJ) tree. **B** Maximum-likelihood (ML) tree. Only bootstrap values ≥ 50% (based on 1,000 replicates) are indicated at the nodes

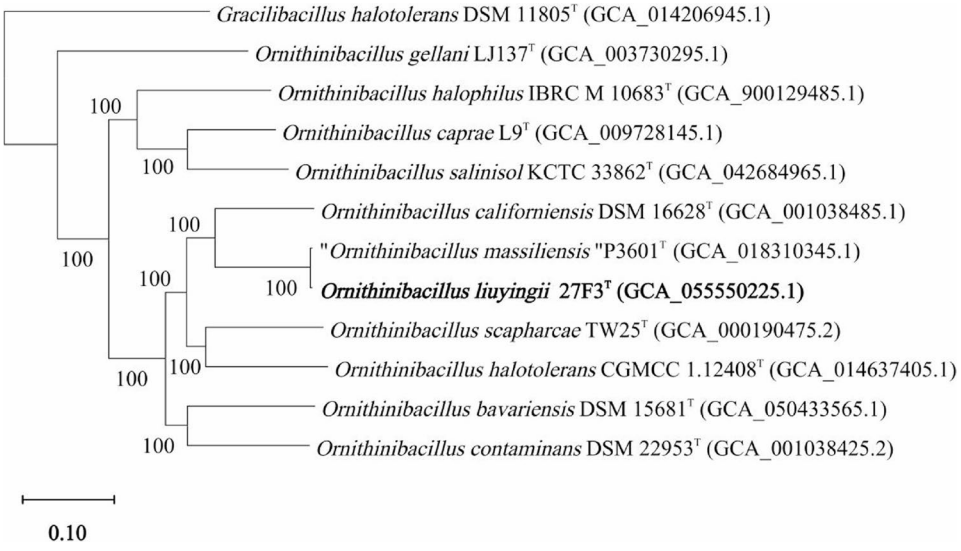

Fig. 3 Phylogenetic analysis based on 92 core-genes of strain 27F3^T and related taxa

Ornithinibacillus. The strain showed a close phylogenetic relationship to *O. californiensis* MB-9^T, yet with sufficient genetic distance to justify its classification as a novel species. All major nodes in the tree were strongly supported, demonstrating a highly reliable phylogenetic topology consistent with the current taxonomy of the genus. These core-gene-based phylogenetic results provide strong support for the proposal of *Ornithinibacillus liuyingii* sp. nov. with 27F3^T as the type strain.

Genome architecture, mobile genetic elements, and adaptive traits

De novo assembly genome of strain 27F3^T generated 27 scaffolds (comprising 29 contigs), with an N50 of 265,010 bp. These scaffolds were subsequently ordered and merged into a single, complete circular chromosome of 3,801,052 bp with a DNA G+C content of 37.0%. The final assembly was found to be 100% complete with only 0.88% contamination based on CheckM analysis. A total of 3,737 protein-coding genes was predicted, representing a coding density of 84.97%. No plasmids were identified. The annotated genome map generated with Prokka is presented in Fig. 4A, with coding sequences colored according to functional categories (including tmRNA, tRNA, and rRNA), and selected genes labeled.

Analysis of mobile genetic elements revealed two CRISPR arrays identified via CRISPRCasFinder, both assigned with the highest confidence score (evidence level 1). The first CRISPR locus spans nucleotides 69,363–69,531 bp, containing a 55 bp repeat and one 59 bp spacer. The second array is located between positions 235,444–235,553 bp, with a 28 bp repeat and a 54 bp spacer. No *cas* gene clusters were detected in proximity to these arrays, suggesting an inactive or acquired CRISPR system; however, their presence indicates past viral encounters.

A putative prophage region was predicted using PHASTER, spanning 14,475 bp (from 60,942 to 75,416 bp). This region was assessed as "low-quality"

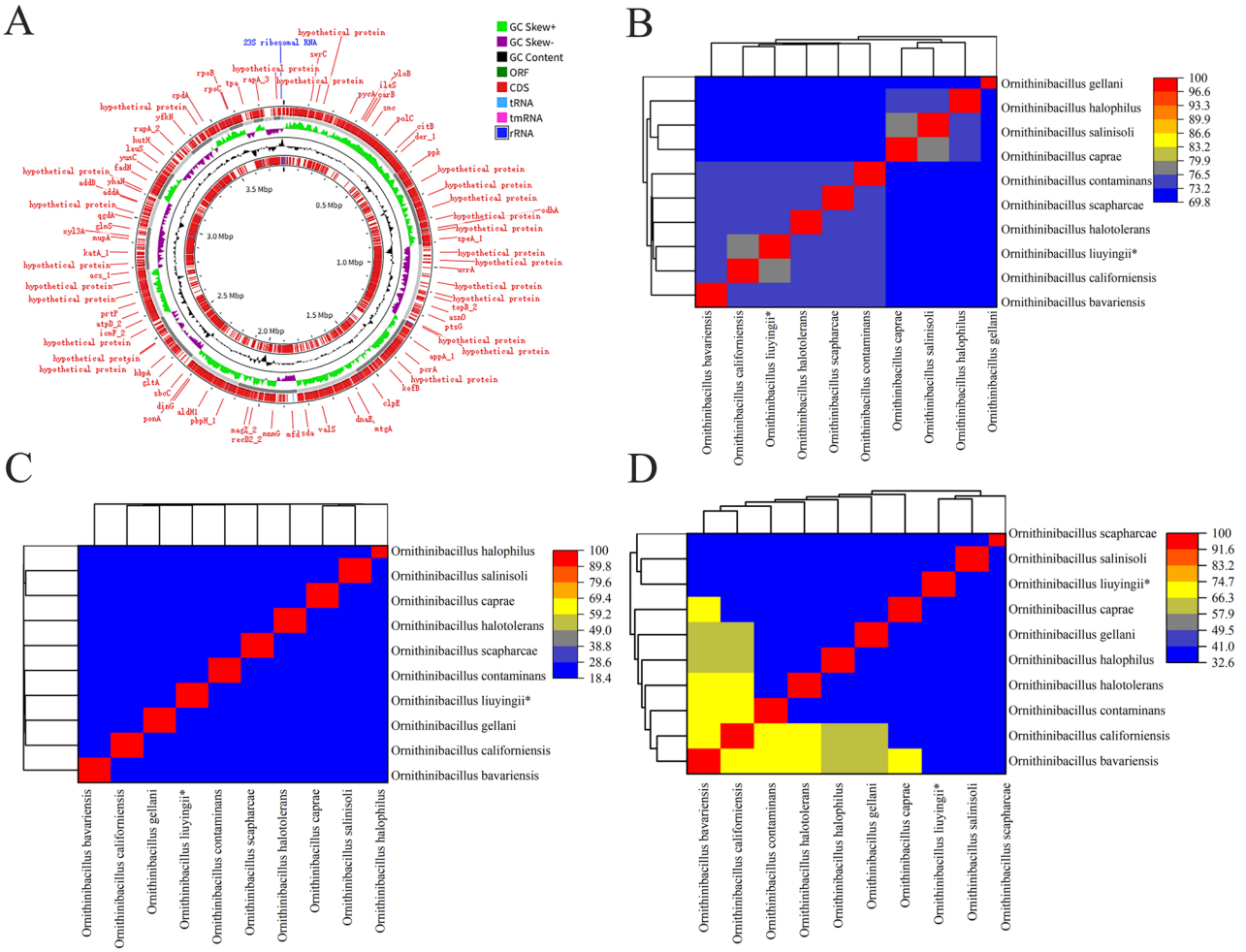

Fig. 4 Genomic and chemotaxonomic features of strain 27F3^T. **A** Circular genome map. **B** Cluster heatmap of ANI values. **C** Cluster heatmap of dDDH values. **D** Cluster heatmap of AAI values

with an estimated completeness of 24.18%, implying a partially retained or degraded prophage. Among its 16 predicted genes, 10 displayed identities to viral proteins, and one was likely host-derived. Although unlikely to produce infectious particles, this region may contribute to genomic variation or regulatory adaptation.

Genomic taxonomy and phylogenomic delineation

Taxonomic classification based on the genome assembly of strain 27F3^T was conducted with GTDB-Tk using the reference database release r214. The strain was assigned to the genus *Ornithinibacillus* (replacing the invalidly published name *Paucisalibacillus*), with the closest validly published type strain being *O. californiensis*, showing an ANI of 79.67% and an alignment fraction (AF) of 0.383. This ANI value is well beneath the accepted species threshold of 95–96%, supporting the designation of strain 27F3^T as a novel species within the genus.

Notably, this genomic assignment contrasts with the previous 16S rRNA gene-based identification, in which BLAST analysis indicated the highest similarity (98.5%) to *O. scapharcae* TW25^T and 97.7% to *O. californiensis*. This discrepancy may underscore the limitations of relying solely on 16S rRNA gene sequence identity for species-level classification and emphasizes the necessity of whole-genome sequencing for robust phylogenetic inference.

To further resolve its taxonomic status, ANI and dDDH analyses were performed against all validly published *Ornithinibacillus* species with available genomes (9 of 10; *O. heyuanensis* was excluded due to lack of genomic data). The ANI values all fell below 76.98%, with the highest match to *O. californiensis*, followed by *O. halotolerans* (75.02%) and *O. scapharcae* (75.01%) (Fig. 4B). Similarly, dDDH values were all below 21.9%, with the highest relatedness to *O. gellani* (21.9%), *O. californiensis* (20.9%), and *O. caprae* (19.8%) (Fig. 4C). These results collectively indicate that strain 27F3^T represents a novel species of the genus *Ornithinibacillus*. Consistent with the ANI and dDDH findings, the AAI values observed between strain 27F3^T and its closest relatives were 30–38.85%, supporting its classification as a novel species (Fig. 4D).

Comparative genomic analyses based on ANI, dDDH, and AAI yielded values of 99.11%, 93.10%, and 99.13%, respectively, between strain 27F3^T and the "*Ornithinibacillus massiliensis*" strain. These results indicate that the two strains belong to the same species.

Physiological characteristics

Physiological characterization of strain 27F3^T was conducted using Biolog GEN III microplates, API 50CHB, API ZYM, and API 20NE test systems. The strain grew at temperatures ranging from 20 to 45 °C, tolerated NaCl concentrations of 0–8% (w/v), and exhibited motility under the tested conditions. Although these traits were consistent with related species including *O. scapharcae*, *O. californiensis*, *O. bavariensis*, and *O. contaminans*, several distinctive phenotypic features were observed [40]. These included weakly positive utilization of *α*-D-glucose and D-mannose, positive assimilation of xylitol, and detectable *β*-glucosidase activity. In the API 20NE system, the strain tested positive for esculin hydrolysis (indicating *α*-glucosidase activity) and gelatin hydrolysis, while all other tests in the kit yielded negative results. These metabolic characteristics may serve as diagnostic traits differentiating strain 27F3^T from other recognized *Ornithinibacillus* species (Table 1).

Chemotaxonomic properties

The major cellular fatty acids of strain 27F3^T were identified as iso-$C_{15:0}$ (43.6%), anteiso-$C_{15:0}$ (16.7%), and iso-$C_{17:0}$ (12.8%). Comparative analysis with closely related species (*O. scapharcae*, *O. californiensis*, *O. bavariensis*, and *O. contaminans*) revealed relatively elevated proportions of $C_{18:1}$ *ω9c* (0.8%), iso-$C_{14:0}$ (2.9%), and iso-$C_{16:0}$ (5.3%) (Table 2) [40]. Menaquinone-7 (MK-7) constituted the predominant respiratory quinone, with minor quantities of MK-8. Polar lipid profiling indicated the presence of diphosphatidylglycerol (DPG), phosphatidylethanolamine (PE), phosphatidylglycerol (PG), along with several unidentified phospholipids (PL) and glycolipids (GL).

Genome functional annotation

KEGG annotation

A total of 3,429 genes with functional domains were identified (Fig. 5A), revealing a complete sporulation pathway (spore coat proteins CotO/CotZ, germination receptor GerA, spore transporters SpoVAC/SpoVAEB/SpoVAD, regulators SpoIIE/SpoVS, cell division proteins SpoIID/FtsL), diverse metabolic systems (F420-dependent oxidoreductase, cytochromes COX1/2/3, cytochrome C, Fe-S cluster assembly, molybdenum cofactor synthesis MoaE, cobalamin transport ABC_cobalt, lipid-modifying acetyltransferases, multidrug efflux pumps), secretion/transport machinery (ABC transporters ABC_tran/ABC_membrane, type IV pili TadE, type II secretion T2SSE/F, flagellar proteins FliG/FliM/FlgD), stress response components (nucleases RNase_H/exonuclease, radical detoxifier Radical_SAM, heat shock protein HSP20), transcriptional regulators (TetR, MerR, Sigma70 family), two-component systems (HisKA kinase, response regulators), and virulence-associated genes (hemolysin HlyIII, cell wall hydrolases LysM/Amidase_3, biofilm protein LytTR) (Supplementary Table S1).

COG annotation

The analysis of COG functional categories (Fig. 5B) corroborated these findings and further identified

Table 1 Physiological characteristics that differentiate strain 27F3T from other closely related species

Strains	27F3^T	*O.scapharcae* TW25^T	*O. californiensis* DSM 16,628^T	*O. bavariensis* DSM 15,681^T	*O. contaminans* DSM 22,953^T
Temperature range	20–45	10–37	10–37	15–45	20–45
Optimal temperature	30	30	30	42	30
Salinity range (%, w/v)	0–8.0	0–5.0	0.5–12.0	0–10.0	0–6.0
Optimal salinity (%, w/v)	0.5–4.0	1.0	0.5–8.0	0.5–4.0	0
Motility	+	+	+	+	–
Carbon source (BIOLOG GENIII)					
a-D-Glucose	w	–	–	–	+
D-Mannose	w	–	–	–	+
Salicin	+	-	+	–	–
Sucrose	-	–	w	–	–
D-Trehalose	w	–	+	–	w
L-Malic acid	-	–	w	–	–
Pyruvatic acid methyl ester	-	–	–	w	–
Acid production from(API 50CHB)					
Glycerol	w	+	+	+	w
D-Arabinose	–	–	–	–	w
D-Ribose	–	+	w	+	–
D-Xylose	–	w	–	–	+
D-Fructose	+	–	–	+	w
D-Mannose	–	–	–	–	+
D-Mannitol	+	+	–	+	w
D-Sorbitol	–	–	–	w	–
Methyl-a-D-glucoside	–	w	–	–	+
N-Acetylglucosamine	–	+	–	+	+
Amygdalin	+	+	–	–	w
Arbutin	–	+	–	–	w
Salicin	+	+	+	–	+
D-Cellobiose	+	+	–	w	+
D-Maltose	+	+	+	–	+
Sucrose	–	+	+	–	–
D-Trehalose	+	+	+	w	+
Starch	+	+	w	–	+
Glycogen	–	+	–	–	–
Xylitol	+	w	–	w	w
Gentiobiose	–	w	–	–	w
D-Arabitol	–	–	–	w	+
5-Ketogluconate	–	–	w	w	w
Enzyme activity(API ZYM)					
Alkaline phosphatase	+	+	–	+	–
Esterase (C4)	+	+	+	w	+
Esterase lipase (C8)	+	w	+	w	w
Leucine arylamidase	+	w	w	+	w
Acid phosphatase	+	–	–	+	–
Naphthol-AS-BI-phosphohydrolase	+	w	w	+	w
a-Glucosidase	+	+	+	–	+
β-Glucosidase	+	w	–	–	–
API 20NE					
Esculine citrate de fer	+	n	n	n	n
Gelatine	+	n	n	n	n

"+", positive, "*w*" weakly positive, "–" negative, "*n*" no test

Table 2 Cellular fatty acid profiles (%) of strain 27F3T and the reference species

Fatty acid	27F3^T	*O. scapharcae* TW25^T	*O. californiensis* DSM 16,628^T	*O. bavariensis* DSM 15,681^T	*O. contaminans* DSM 22,953^T
Saturated acids					
$C_{10:0}$	-	tr	tr	tr	0.5
$C_{12:0}$	tr	-	-	-	0.6
$C_{14:0}$	1.0	4.4	0.5	0.6	1.1
$C_{15:0}$	-	0.6	tr	tr	-
$C_{16:0}$	4.5	11.8	1.8	3.0	1.8
$C_{18:0}$	tr	-	-	tr	-
Unsaturated acids					
$C_{16:1}\omega 11c$	tr	tr	3.2	1.3	-
$C_{16:1}\omega 7c$ alcohol	tr	-	3.1	0.8	-
$C_{18:1}\omega 7c$	-	-	-	tr	-
$C_{18:1}\omega 9c$	0.8	-	-	tr	-
Branched acids					
iso-$C_{11:0}$	-	-	-	tr	-
iso-$C_{13:0}$	0.6	1.0	tr	tr	0.7
iso-$C_{14:0}$	2.9	0.9	1.1	1.0	1.5
iso-$C_{15:0}$	43.6	56.1	43.4	46.6	46.6
iso-$C_{15:0}$ iso 3OH	tr	tr	-	-	-
anteiso-$C_{15:0}$	16.7	15.2	22.2	17.5	17.4
iso-$C_{16:0}$	5.3	1.2	1.4	2.9	4.8
iso-$C_{17:0}$	12.8	5.1	5.9	9.8	13.0
anteiso-$C_{17:0}$	10.4	4.1	8.8	10.8	12.1
iso-$C_{17:1}\omega 10c$	tr	-	3.1	2.7	-
Summed feature 3	tr	tr	-	-	-
Summed feature 4	tr	-	4.8	1.2	-

all values are percentages of total fatty acids. "*tr*" trace (< 0.5%)

"-" not detected. Summed feature 3 comprises C16:1 *ω*7c/C16:1 *ω*6c; Summed feature 4 comprises C17:1 iso I/anteiso B

core metabolic pathways (pyruvate dehydrogenase COG0022/1071, TCA cycle COG0373/0538, FoF1-ATP synthase COG0055/0056, quinone synthases COG2226), genetic information processes (DNA replication/repair COG0587/2812/0249/0323, transcription COG1595/1758, translation COG0018/0013/0199/0333, nucleotide metabolism COG0046/0047/0503/0494/1051), a specialized sporulation system spanning initiation (Spo0F COG5803, Spo0A COG5801, Sda COG5851), maturation (SpoVB COG5841, SleL COG3858, CotE/CotD COG5880/5879, Ssp family COG5852), and germination (GerA COG5901, Gpr COG5911, YpeB COG5914), stress adaptation mechanisms (multidrug efflux COG1132/1131, metal transport COG2239/0803, osmoprotection COG1292, detoxification enzymes COG0753/1225/1230/1051, cold shock protein COG1278, HSP90 COG0326, universal stress protein COG0589), and unique traits including molybdenum cofactor synthesis (COG2896-0315), bacillithiol synthase (COG4365), Tat secretion (COG1826), uncharacterized proteins (DUF families COG2323/4129, conserved proteins COG4471/4841), and regulatory diversity (MerR/MarR COG0789/1846, c-di-GMP metabolism COG5001, quorum sensing LuxS COG1854) (Supplementary Table S2).

NR database identity

Among the 3,407 predicted genes, the majority showed highest similarity to sequences from *Ornithinibacillus* species (Fig. 6A): 1,639 genes (48.11%) matched unclassified *Ornithinibacillus* sp., 1,299 genes (38.13%) matched *Ornithinibacillus* sp. BX22, and 359 genes (10.54%) matched *Ornithinibacillus massiliensis*. Collectively, these three taxa accounted for 96.78% of annotated genes, supporting close phylogenetic affinity to *Ornithinibacillus*, particularly to unclassified members and strain BX22. The remaining 110 genes (3.22%) showed similarity to sequences from other generam including *Paucisalibacillus* sp., *Oceanobacillus* sp., and *Bacillus* sp. (Supplementary Table S3).

PHI-base annotation

A total of 395 host-interaction genes were identified (Fig. 6B), comprising 234 (59.24%) "reduced virulence" genes, 90 (22.78%) "unaffected pathogenicity" genes, and 47 (11.90%) "increased virulence" genes. Additional categories included 12 genes (3.04%) linked with "loss

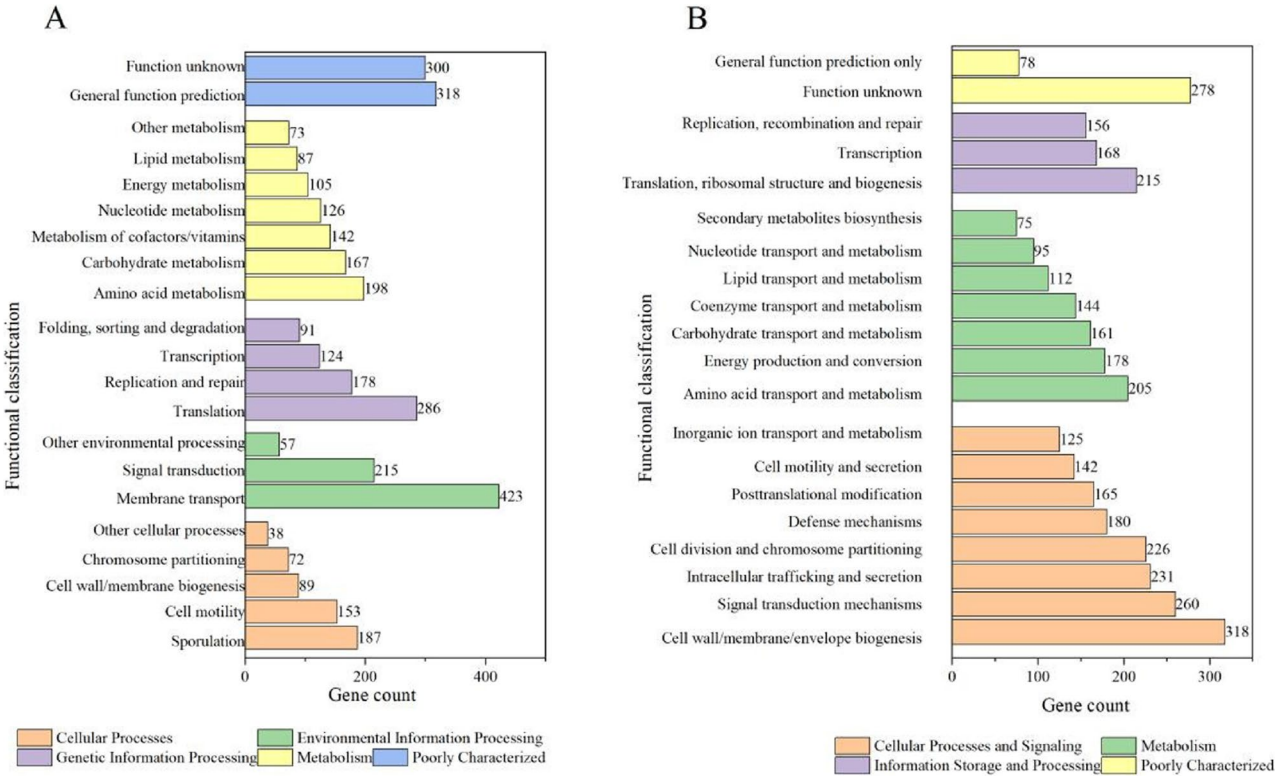

Fig. 5 Functional genome annotation of strain 27F3^T. **A** KEGG pathway distribution. **B** COG functional categories

of pathogenicity", 7 "lethal" genes (1.77%), 3 plant effector genes, and 2 chemical target genes mediating chemical sensitivity or resistance (0.25% each) (Supplementary Table S4).

VFDB virulence profiling

Over 100 virulence-associated genes were annotated (Fig. 6C), functionally spanning capsule biosynthesis (*cps4I*, *cpsB*, *wbtE*, core components *cpsA/uppS* and *cpsD*), motility/adhesion systems (*flagellar fliI*, *flgC*, *motA; pilin pilT*), immune evasion factors (*hlyIII*, *sodB/sodC*, *katA*), iron acquisition machinery (*vctC*, *fbpC*, *irtB*), regulatory networks (*virR*, *cheY*, *phoP*, *regX3*), and effector secretion systems (T4SS components *lirB*, *ricA*, *dot/icm*). Sequence identity to reference virulence factors reached up to 83.3% for genes enriched in capsule synthesis pathways (*LytR* regulators), sugar metabolism (*galU*, *ugd*), and proteolytic functions (*Clp* proteases) (Supplementary Table S5).

Comparison of 16S rRNA gene amplicon sequencing results

The 16S rRNA gene amplicon sequencing analysis yielded a total of 5,121 microbial taxa. The V3–V4 region of strain 27F3^T was compared against these sequences. Under 100% query coverage, the highest identity value obtained was 95.80%. According to the criterion that a 16S rRNA gene similarity threshold of 98.7% or higher is typically required to preliminarily identify strains as the same species [6], this suggests that the novel strain 27F3^T is likely not present in the lung tissues of the examined rodent species (*A. chevrieri*, *Rattus losea*, and *Niviventer confucianus*), or that the V3–V4 region of the 16S rRNA gene is too short, leading to limitations in resolution. A detailed analysis of the reasons for this is provided in the Discussion section below.

Antibiotic susceptibility profile of strain 27F3^T

The antimicrobial susceptibility profile of strain 27F3^T was determined by broth microdilution against a panel of 30 antibiotics. The isolate exhibited susceptibility to a broad range of agents, including β-lactam/β-lactamase inhibitor combinations (e.g., ampicillin/sulbactam, MIC ≤ 1 μg/mL; amoxicillin/clavulanic acid, MIC ≤ 1 μg/mL), carbapenems (imipenem, MIC 0.5 μg/mL; meropenem, MIC ≤ 0.12 μg/mL; ertapenem, MIC ≤ 0.25 μg/mL), third-generation cephalosporins (ceftazidime, MIC ≤ 0.5 μg/mL; cefotaxime, MIC ≤ 0.12 μg/mL), aminoglycosides (gentamicin, MIC ≤ 1 μg/mL; amikacin, MIC ≤ 4 μg/mL), chloramphenicol (MIC ≤ 2 μg/mL), tetracyclines (including tigecycline, MIC ≤ 0.25 μg/mL), fluoroquinolones (ciprofloxacin, MIC 0.12 μg/mL), as well as azithromycin (MIC ≤ 2 μg/mL) and cotrimoxazole (MIC ≤ 0.25 μg/mL) (Table 3).

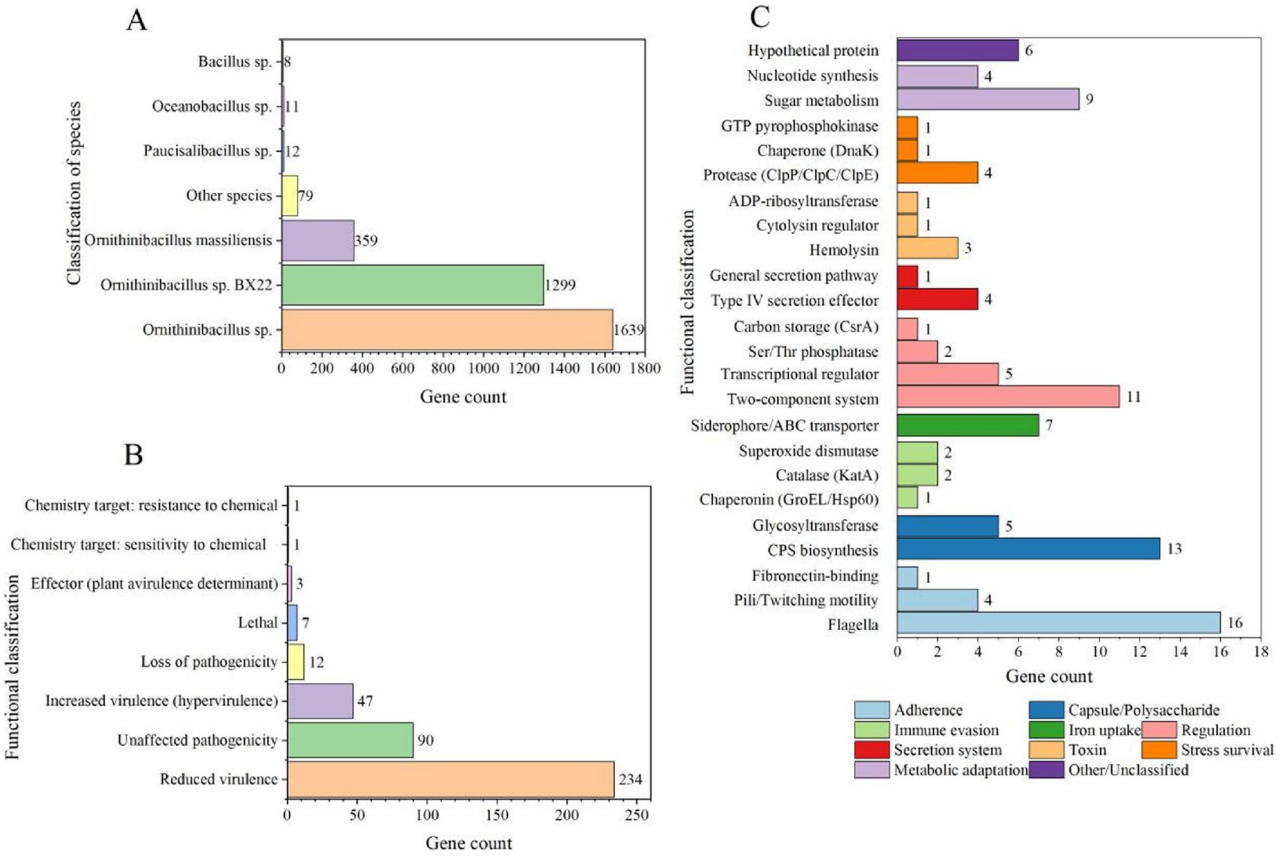

Fig. 6 Comparative genomic analysis of strain 27F3^T. **A** NR database identity. **B** PHI-base pathogen-host interaction genes. **C** VFDB virulence factor annotation

Notably, strain 27F3^T demonstrated resistance to nalidixic acid (MIC 64 μg/mL) and polymyxin E (colistin, MIC 8 μg/mL), and displayed intermediate susceptibility to polymyxin B (MIC 2 μg/mL). Given that nalidixic acid and polymyxins are primarily effective against Gram-negative bacteria due to their mechanisms of action (inhibition of DNA gyrase/topoisomerase IV and disruption of the outer membrane, respectively), and considering that *Ornithinibacillus* is a genus comprising predominantly Gram-positive members, the observed resistance to these agents in strain 27F3^T (which phenotypically presents as Gram-negative) is an expected characteristic and aligns with the typical intrinsic resistance profile of Gram-positive bacteria toward these drug classes.

Furthermore, strain 27F3^T was resistant to cefepime (a fourth-generation cephalosporin, MIC 8 μg/mL), while remaining susceptible to other tested β-lactams, including third-generation cephalosporins and carbapenems (Table 3). This specific resistance pattern suggests a mechanism distinct from broad-spectrum β-lactamase production, which was not detected genomically. Intrinsic resistance to certain cephalosporins is known in some Gram-positive bacteria within the order *Caryophanales*, such as *Listeria* spp., attributed to the low affinity of their penicillin-binding proteins (PBPs) for these antibiotics. The resistance to cefepime observed in strain 27F3^T may involve a similar PBP-based mechanism, reduced permeability, or specific efflux activity, warranting further investigation.

Discussion

Description of *Ornithinibacillus liuyingii* sp. nov.

Ornithinibacillus liuyingii (liu.ying'i.i. N.L. gen. n. *liuyingii*, of Dr. Ying Liu, an outstanding microbiologist from Guizhou Province, in recognition of her significant contributions to the prevention and control of *Leptospirosis*).

Cells are Gram-negative, motile, and rod-shaped. Colonies grown on Columbia blood agar are greyish-light purple with concentric circles and exhibit no hemolytic activity. Optimal growth occurs at 30 °C (range 20–45 °C) and 0.5–4% NaCl (range 0–8%, w/v). Positive for esculin hydrolysis and gelatin hydrolysis. Major cellular fatty acids iso-$C_{15:0}$, anteiso-$C_{15:0}$, and iso-$C_{17:0}$; the major respiratory quinone is menaquinone-7 (MK-7); polar lipids consist of diphosphatidylglycerol, phosphatidylethanolamine, phosphatidylglycerol, and glycolipids.

Strain 27F3^T (= GDMCC 1.5626^T = JCM 38003^T) was isolated from the intestinal contents of *A. chevrieri*, a

Table 3 The antibiotic sensitivity test results of strain 27F3T

Antibiotic name	Abbreviation	Concentration range (μg/mL)	MIC (μg/mL)	Results
Ampicillin	AMP	1–64	<=1	S
Ampicillin/sulbactam	A/S2(AMS)	1/0.5–64/32	<=1	S
Cefoxitin	CFX	1–64	<=1	S
Cefuroxime	CXM	1–64	<=1	S
Cefepime	CPM	1–32	8	**R**
Ceftazidime	CAZ	0.5–32	<=0.5	S
Ceftazidime/clavulanic acid	CAZ/C	0.25/4–16/4	<=0.25	S
Cefotaxime	CTX	0.12-8	<=0.12	S
Cefotaxime/clavulanic acid	CTX/C	0.06/4–4/4	<=0.06	S
Chloramphenicol	CHL	2–64	<=2	S
Polymyxin E	CT	0.25-8	8	**R**
Ciprofloxacin	CIP	0.015-32	0.12	S
Nalixic acid	NAL	2–64	64	**R**
Cefazolin	CFZ	1–32	<=1	S
Ceftiofur	CEF	0.5–16	<=0.5	S
Ceftazidime/avibactam	CZA	0.5/4–16/4	<=0.5	S
Imipenem	IPM	0.25-8	0.5	S
Ertapenem	ETP	0.25-8	<=0.25	S
Amoxicillin/clavulanic acid	AMC	1/0.5–64/32	<=1	S
Gentamicin	GEN	1–32	<=1	S
Amikacin	AMK	4–64	<=4	S
Streptomycin	STR	4–32	<=4	S
Tetracycline	TET	1–32	<=1	S
Meropenem	MEM	0.12-4	<=0.12	S
Tigacycline	TIG	0.25-8	<=0.25	S
Polymyxin B	PB	0.25-8	2	**I**
Azithromycin	AZM	2–64	<=2	S
Cotrimoxazole	SXT	0.5/9.5-8/152	<=0.25	S
Flufenicol	FFC	1–32	2	S

"*R*" indicates resistant, "*S*" indicates sensitive, "*I*" indicates intermediate

rodent from the Guizhou Plateau. The genomic DNA G + C content is 37.0%. The GenBank accession numbers for the 16S rRNA gene and whole genome sequences of strain 27F3^T are PV917722 and JBPWOS000000000, respectively.

Public health significance

In 2017, "*Ornithinibacillus massiliensis*" was isolated from faecal samples of malnourished children in Africa, though it remains listed as "not validly published" on the LPSN website [39]. To date, this single report remains the only documentation of this species. In the present study, we identified this bacterium in lung tissue of *Apodemus chevrieri* from Southwest China. Using a polyphasic taxonomic approach, we propose to identify it as *Ornithinibacillus liuyingii* sp. nov., providing a detailed taxonomic description, genomic characteristics, and evidence of its antimicrobial resistance phenotype. The isolation of strain 27F3^T from a mammalian lung, together with a prior report of a closely related *Ornithinibacillus* strain from human fecal samples [39], may prompt consideration of its ecological range and potential host associations. Phenotypic and genotypic analyses revealed a distinctive antimicrobial resistance profile and the presence of numerous genes homologous to known virulence and resistance determinants. While these genomic features warrant attention, it is important to note that their presence alone does not confirm functional expression, pathogenicity, or clinical risk. The phenotypic resistance observed (e.g., to nalidixic acid, polymyxins, and cefepime) appears largely consistent with intrinsic mechanisms expected for its phylogenetic lineage, as discussed below. Therefore, the direct public health significance of *O. liuyingii* remains to be determined and would require dedicated studies on its pathogenicity, transmissibility, and the functional validation of its annotated genetic repertoire.

Genomic features and potential adaptations

Genome annotation of *O. liuyingii* revealed genetic signatures that may be interpreted in the context of its isolation environment. The genome encodes a complete sporulation gene cluster (conserved with *Bacillus subtilis* [41]), including homologs of spore coat proteins such as CotZ [42]. Sporulation is a survival strategy common in the family *Bacillaceae* and may confer an advantage in fluctuating environments. Additionally, genes associated with oxidative stress response, including superoxide dismutase (*sodB*) and catalase (*katA*) [43], were identified. While such genes are widespread among bacteria, their presence could theoretically contribute to survival under conditions of increased oxidative stress, such as those encountered in high-altitude environments with intense UV radiation—a strategy observed in other bacteria from

similar niches [44]. However, we emphasize that these genomic predictions are suggestive of potential adaptive traits; conclusive evidence for high-altitude adaptation would require comparative physiological assays under controlled environmental conditions. Similarly, the detection of flagellar assembly genes correlated with the observed motility, a common phenotypic trait.

Interpretation of the antimicrobial resistance phenotype

The antimicrobial susceptibility profile of *O. liuyingii* 27F3^T presents a distinctive pattern that merits discussion in light of its unique taxonomic position. Notably, the strain exhibited resistance to nalidixic acid and polymyxins (colistin and polymyxin B), while demonstrating susceptibility to a broad range of other antibiotic classes. This pattern is consistent with fundamental principles of antimicrobial action and the phylogenetic context of the isolate. Nalidixic acid, a first-generation quinolone, primarily targets DNA gyrase in Gram-negative bacteria and demonstrates inherently poor activity against most Gram-positive organisms due to differences in target enzyme susceptibility and cellular permeability barriers [45]. Similarly, the polymyxin class exerts its bactericidal effect by binding to lipopolysaccharide (LPS) in the outer membrane of Gram-negative bacteria; their characteristic inactivity against Gram-positive bacteria, which lack an outer membrane and LPS, is a well-established pharmacological trait [46]. Therefore, the observed resistance of the predominantly Gram-positive genus *Ornithinibacillus* to these agents may be considered an expected intrinsic characteristic, further supporting the strain's phylogenetic placement despite its atypical Gram-negative staining morphology.

A more intriguing finding is the specific resistance to cefepime (a fourth-generation cephalosporin) alongside retained susceptibility to other β-lactams, including third-generation cephalosporins and carbapenems. This selective resistance profile is not typical of broad-spectrum β-lactamase activity. Instead, it mirrors the well-documented intrinsic resistance pattern observed in Listeria species (order Caryophanales), which are uniformly resistant to cephalosporins yet remain susceptible to penicillins and carbapenems [47]. This resistance in Listeria is not mediated by β-lactamase production but is attributed to the low binding affinity of its essential penicillin-binding proteins (PBPs), particularly PBP3, for cephalosporin antibiotics [48, 49]. By analogy, the cefepime-specific resistance in *O. liuyingii* 27F3^T may plausibly stem from a similar, inherently non-susceptible PBP profile or other non-enzymatic mechanisms such as reduced drug penetration. This phenotype underscores that susceptibility patterns in environmental bacteria, especially those occupying novel phylogenetic niches, can deviate from conventional expectations and may reflect deep-seated physiological or structural adaptations [50]. The comprehensive susceptibility testing performed here highlights the necessity of such profiling for accurate characterization of novel species.

Genomic features and virulence gene homologs

Bioinformatic annotation of the *O. liuyingii* genome identified numerous genes encoding products homolous to known bacterial virulence factors, such as proteins involved in capsule biosynthesis, hemolysin production, and pilus assembly [51, 52]. The presence of such genetic homologs in a bacterium isolated from wildlife may underscore the vast and untapped genetic diversity within environmental and animal-associated microbiomes. However, sequence homology alone does not confer a pathogenic phenotype. The functional role and expression of these genes in *O. liuyingii* remain unknown. This finding is consistent with the results of the PHI-base analysis, which classified the majority of predicted host-interaction genes in the "reduced virulence" category. This pattern highlights the complex and often attenuated nature of virulence-associated gene inventories in environmental bacteria, where such sequences may serve non-pathogenic, ecological functions or represent evolutionary relics. The genomic landscape of strain 27F3^T also includes common features such as CRISPR arrays and a partial prophage region, indicating a history of phage interactions that may contribute to the genomic plasticity typical of many bacterial species.

Considerations on the atypical gram reaction of *O. liuyingii*

The consistent Gram-negative reaction of strain 27F3^T, as determined by both conventional staining and the KOH test, may represent a notable phenotypic deviation from all other described *Ornithinibacillus* species. Such discordance between Gram stain phenotype and phylogenetic expectation, while uncommon, is documented in other bacterial groups and can arise from several factors, including alterations in cell wall thickness, peptidoglycan composition, or the presence of additional surface layers that affect dye retention [53, 54].

In the case of *O. liuyingii*, the TEM observations of a thick, electron-dense cell wall and the lack of genomic evidence for a complete LPS biosynthesis pathway suggest that it is not a typical diderm (Gram-negative) bacterium possessing a definitive outer membrane. It is more plausible that the observed staining phenotype results from a modified cell wall architecture within the monoderm (Gram-positive) lineage. Potential explanations may include a comparatively thinner or less cross-linked peptidoglycan layer than that of its relatives, or the presence of surface compounds that impede the retention of the crystal violet-iodine complex. We therefore propose that *O. liuyingii* is best described as a Gram-stain-negative

member of a Gram-positive genus, emphasizing the methodological outcome while acknowledging its likely monoderm phylogenetic identity. This finding highlights the limitations of relying solely on Gram staining for definitive cell wall classification and underscores the importance of integrating ultrastructural and genomic data.

Interpretation of 16S rRNA gene amplicon sequencing analysis

The isolation and identification of a novel *Ornithinibacillus* species (strain 27F3^T) from the lung tissue of *A. chevrieri* may represent a significant contribution to the understanding of bacterial diversity in rodent respiratory systems. However, subsequent 16S rRNA gene amplicon sequencing (V3–V4 region) of lung tissues from 90 wild rodents (including 30 *A. chevrieri*, 30 *Rattus losea*, and 30 *Niviventer confucianus*) revealed a maximum sequence identity of only 95.8% with the 27F3^T strain under 100% query coverage. This low similarity suggests that the novel bacterium is not a common colonizer of the rodent lung microbiome in the sampled population. Several factors may explain this discrepancy.

First, the low detection rate and sequence similarity may indicate that strain 27F3^T is not a resident member of the core lung microbiota but rather a transient or environmentally acquired bacterium. Rodents are known to be exposed to diverse environmental microbes through foraging, burrowing, and respiratory activities. Although strict aseptic techniques were followed during dissection and DNA extraction, the possibility of accidental environmental contamination during animal capture or handling cannot be entirely ruled out. Moreover, the bacterium might have been present in low abundance or only in a subset of individuals, making its detection challenging with amplicon sequencing alone. Second, limitations inherent to 16S rRNA gene amplicon sequencing may have contributed to the low identity score. The V3–V4 region, while widely used for microbial community profiling, has limited resolution at the species level due to sequence conservation across closely related taxa [55]. This is particularly relevant for novel species within poorly characterized genera such as *Ornithinibacillus*, where reference databases may lack representative sequences. Additionally, PCR bias, primer mismatches, and sequencing errors can further reduce the accuracy of matches to known sequences [56]. Third, ecological and host-specific factors may influence bacterial colonization. *Ornithinibacillus* species are often associated with soil, marine environments, or invertebrates, and their presence in mammalian lungs may be accidental rather than symbiotic. The lung environment, with its immune surveillance and clearance mechanisms (e.g., mucociliary clearance), may not provide a suitable niche for sustained colonization by such bacteria [57]. Furthermore, host species differences in immune function or lung physiology could explain why the bacterium was detected only in a single individual of *A. chevrieri* and not in *R. losea* or *N. confucianus*. Finally, the timing of sample collection and processing, though conducted promptly, may not have preserved viable or DNA-intact bacteria if the bacterium was in a state of decay or stress at the time of capture. Future studies could employ metagenomic sequencing or species-specific quantitative PCR to improve detection sensitivity and confirm the prevalence of strain 27F3^T.

In conclusion, while strain 27F3^T represents a valid novel species based on whole-genome and biochemical analyses, its absence in the amplicon sequencing data may suggest it is not a common constituent of the rodent lung microbiome. Its original detection may reflect transient exposure or rare colonization events rather than stable symbiosis.

Conclusion

O. liuyingii may represent a novel species within the genus *Ornithinibacillus*, primarily distinguished by its consistent Gram-stain-negative phenotype, a notable exception within this otherwise Gram-positive genus. Polyphasic taxonomic analyses, including phylogenomics, low ANI/dDDH values, and distinct chemotaxonomic profiles, provide robust support for its status as a novel species. Genomic analysis revealed traits, such as sporulation and oxidative stress response genes, that may contribute to persistence in its isolation environment. Furthermore, the genome encodes homologs of various virulence-associated factors, although their functional role and any pathogenic potential remain unknown. The specific antimicrobial resistance profile, particularly to resistance to cefepime, may add to its distinctive phenotypic characterization. The discovery of *O. liuying*ii expands the known ecological and phenotypic diversity of the genus, illustrating the unexpected complexity within wildlife-associated microbiota. Future studies should focus on elucidating the ultrastructural basis of its atypical Gram-stain reaction, functionally characterizing its genomic adaptations, and monitoring the prevalence and genomic context of such bacterial lineages in environmental and animal hosts to better understand their ecological role and any long-term public health significance within a One Health framework.

Supplementary Information

The online version contains supplementary material available at https://doi.org/10.1186/s12866-026-04949-1.

Supplementary Material 1: Table S1. Predicted gene functions of strain 27F3T in KEGG.

Supplementary Material 2: Table S2. Predicted gene functions of strain 27F3T in COG.

Supplementary Material 3: Table S3. Predicted gene functions of strain 27F3T in NR.

Supplementary Material 4: Table S4. Predicted gene functions of strain 27F3T in PHI.

Supplementary Material 5: Table S5. Predicted gene functions of strain 27F3T in VFDB.

Acknowledgements
No.

Authors' contributions
JZ and TG designed the study, conducted the study trial, and drafted the manuscript; YZ, JZZ and XXZ provided samples, and the trial operation; FMC and YH provided technical support for the trial; SJL are the funding source, supervisor, designed the study and revised the manuscript.

Funding
1. Key Laboratory of Microbiol and Infectious Disease prevention &Control in Guizhou Province. Grant No. Qiankehe Platform Talent-ZDSYS [2023] 004;
2. Project for Public Health Talent Cultivation of China. Grant No. Guo Jikong Zong Ren Han [2024] 122;
3. The local science foundation of Guizhou Province guided by the Central Committee of China, No.Qiankehe [2025] 024.

Data availability
The 16S rRNA gene sequence of strain 27F3T has been deposited in GenBank under accession number PV917722; WGS of strain 27F3T has been deposited in GenBank under accession number JBPWOS000000000. The raw sequencing of 16S rRNA gene amplicon sequencing generated in this study were deposited into the National Genomics Data Center (NGDC) and can be downloaded freely at https://ngdc.cncb.ac.cn/gsa/browse/CRA026703. Strain 27F3T can be obtained from Guangdong Microbial Culture Collection Center (GDMCC), Japan Collection of Microorganisms (JCM), The preservation numbers are GDMCC 1.5626T = JCM38003T.

Declarations

Ethics approval and consent to participate
All procedures involving animals were conducted in accordance with international standards for wildlife research. The study protocol, including the methods of capture, anesthesia, and euthanasia, was reviewed and approved by the Ethics Committee of the Guizhou Provincial Center for Disease Control and Prevention (Approval No. G2019-01). As the animals were wild-caught, informed consent from a private owner was not applicable.

Consent for publication
Not applicable.

Competing interests
The authors declare no competing interests.

Received: 22 October 2025 / Accepted: 9 March 2026
Published online: 23 April 2026

References

1. Mayr R, Busse HJ, Wortmann L, et al. *Ornithinibacillus* gen. nov., with the species *Ornithinibacillus bavariensis* sp. nov. and *Ornithinibacillus californiensis* sp. nov. Int J Syst Evol Microbiol. 2006;56(Pt 6):1383–9.
2. Gan L, Zhang H, Long X, et al. *Ornithinibacillus salinisoli* sp. nov., a moderately halophilic bacterium isolated from a saline-alkali soil. Int J Syst Evol Microbiol. 2018;68(3):769–75.
3. Cheviron ZA, Brumfield RT. Genomic insights into adaptation to high-altitude environments. Heredity (Edinb). 2012;108(4):354–61.
4. Chen AL, Guo XG, Ren TG, et al. Infestation and distribution of chigger mites on Chevrieri's field mouse (*Apodemus chevrieri*) in Southwest China. Int J Parasitol Parasites Wildl. 2021;17:74–82.
5. Levin D, Raab N, Pinto Y, Rothschild D, Zanir G, Godneva A, Mellul N, Futorian D, Gal D, Leviatan S, Zeevi D, Bachelet I, Segal E. Diversity and functional landscapes in the microbiota of animals in the wild. Science. 2021;372(6539):eabb5352.
6. Chun J, Oren A, Ventosa A, et al. Proposed minimal standards for the use of genome data for the taxonomy of prokaryotes. Int J Syst Evol Microbiol. 2018;68(1):461–6.
7. Thompson JD, Higgins DG, Gibson TJ. CLUSTAL W: improving the sensitivity of progressive multiple sequence alignment through sequence weighting, position-specific gap penalties and weight matrix choice. Nucleic Acids Res. 1994;22:4673–80.
8. Saitou N, Nei M. The neighbor-joining method: a new method for reconstructing phylogenetic trees. Mol Biol Evol. 1987;4:406–25.
9. Tamura K, Peterson D, Peterson N, Stecher G, Nei M, et al. MEGA5: Molecular Evolutionary Genetics Analysis using maximum likelihood, evolutionary distance, and maximum parsimony methods. Mol Biol Evol. 2011;28:2731–9.
10. Brown J, Pirrung M, McCue LA. FQC Dashboard: integrates FastQC results into a web-based, interactive, and extensible FASTQ quality control tool. Bioinformatics. 2017;33(19):3137–9.
11. Bolger AM, Lohse M, Usadel B. Trimmomatic: a flexible trimmer for Illumina sequence data. Bioinformatics. 2014;30(15):2114–20.
12. Bankevich A, Nurk S, Antipov D, Gurevich AA, Dvorkin M, Kulikov AS, Lesin VM, Nikolenko SI, Pham S, Prjibelski AD, Pyshkin AV, Sirotkin AV, Vyahhi N, Tesler G, Alekseyev MA, Pevzner PA. SPAdes: a new genome assembly algorithm and its applications to single-cell sequencing. J Comput Biol. 2012;19(5):455–77.
13. Walker BJ, Abeel T, Shea T, Priest M, Abouelliel A, Sakthikumar S, Cuomo CA, Zeng Q, Wortman J, Young SK, Earl AM. Pilon: an integrated tool for comprehensive microbial variant detection and genome assembly improvement. PLoS ONE. 2014;9(11):e112963.
14. Parks DH, Imelfort M, Skennerton CT, Hugenholtz P, Tyson GW. CheckM: assessing the quality of microbial genomes recovered from isolates, single cells, and metagenomes. Genome Res. 2015;25(7):1043–55.
15. Schwengers O, Barth P, Falgenhauer L, Hain T, Chakraborty T, Goesmann A. Platon: identification and characterization of bacterial plasmid contigs in short-read draft assemblies exploiting protein sequence-based replicon distribution scores. Microb Genom. 2020;6(10):mgen000398.
16. Couvin D, Bernheim A, Toffano-Nioche C, et al. CRISPRCasFinder, an update of CRISRFinder, includes a portable version, enhanced performance and integrates search for Cas proteins. Nucleic Acids Res. 2018;46(W1):W246–51.
17. Arndt D, Grant JR, Marcu A, et al. PHASTER: a better, faster version of the PHAST phage search tool. Nucleic Acids Res. 2016;44(W1):W16–21.
18. Chaumeil PA, Mussig AJ, Hugenholtz P, Parks DH. GTDB-Tk v2: memory friendly classification with the genome taxonomy database. Bioinformatics. 2022;38(23):5315–6.
19. Seemann T. Prokka: rapid prokaryotic genome annotation. Bioinformatics. 2014;30(14):2068–9.
20. Na S, Kim YO, Yoon S, et al. Up-to-date bacterial core gene set and pipeline for phylogenomic tree reconstruction. J Microbiol. 2018;56(4):280–5.
21. Eddy SR. Accelerated Profile HMM Searches. PLoS Comput Biol. 2011;7(10):e1002195.
22. Katoh K, Standley DM. MAFFT multiple sequence alignment software version 7: improvements in performance and usability. Mol Biol Evol. 2013;30(4):772–80.
23. Jain C, Rodriguez-R LM, Phillippy AM, et al. High throughput ANI analysis of 90K prokaryotic genomes reveals clear species boundaries. Nat Commun. 2018;9(1):5114.
24. McKnight DJE, Wong-Bajracharya J, Okoh EB, Snijders F, Lidbetter F, Webster J, Haughton M, Darling AE, Djordjevic SP, Bogema DR, Chapman TA. *Xanthomonas rydalmerensis* sp. nov., a non-pathogenic member of Group 1 Xanthomonas. Int J Syst Evol Microbiol. 2024;74(3):006294.
25. Tian Z, Lu S, Jin D, Yang J, Pu J, Lai XH, Bai XN, Wu XM, Li J, Wang S, Xu J. *Streptococcus chenjunshii* sp. nov. isolated from feces of Tibetan antelopes. Int J Syst Evol Microbiol. 2019;69(4):1237–43.
26. Volokhov DV, Zagorodnyaya TA, Furtak VA, Nattanmai G, Randall L, Jose S, Gao Y, Eisenberg T, Delmonte P, Blom J, Mitchell KK. *Streptococcus sciuri* sp. nov., *Staphylococcus marylandisciuri* sp. nov. and *Staphylococcus americanisciuri* sp. nov., isolated from faeces of eastern grey squirrel (Sciurus carolinensis). Int J Syst Evol Microbiol. 2023;73:8.
27. Xu Y, Xu X, Lan R, Xiong Y, Ye C, et al. An O island 172 encoded RNA helicase regulates the motility of *Escherichia coli* O157:H7. PLoS ONE. 2013;8(6):e64211.

28. Krejčí E, Kroppenstedt RM. Differentiation of species combined into the *Burkholderia cepacia* complex and related taxa on the basis of their fatty acid patterns. J Clin Microbiol. 2006;44(3):1159–64.
29. Sohlenkamp C, López-Lara IM, Geiger O. Biosynthesis of phosphatidylcholine in bacteria. Prog Lipid Res. 2003;42(2):115–62.
30. Collins MD, Jones D. Distribution of isoprenoid quinone structural types in bacteria and their taxonomic implication. Microbiol Rev. 1981;45(2):316–54.
31. Kanehisa M, Goto S. KEGG: Kyoto Encyclopedia of Genes and Genomes. Nucleic Acids Res. 2000;28(1):27–30.
32. Tatusov RL, Galperin MY, Natale DA, et al. The COG database: a tool for genome-scale analysis of protein functions and evolution. Nucleic Acids Res. 2000;28(1):33–6.
33. Clark K, Karsch-Mizrachi I, Lipman DJ, Ostell J, Sayers EW. GenBank Nucleic Acids Res. 2016;44(D1):D67–72.
34. Urban M, Pant R, Raghunath A, et al. PHI-base: the pathogen–host interactions database. Nucleic Acids Res. 2020;48(D1):D613–20.
35. Liu B, Zheng D, Jin Q, et al. VFDB 2019: a comparative pathogenomic platform with an interactive web interface. Nucleic Acids Res. 2019;47(D1):D687–92.
36. Humphries RM, Ambler J, Mitchell SL, Castanheira M, Dingle T, Hindler JA, et al. CLSI Methods Development and Standardization Working Group Best Practices for Evaluation of Antimicrobial Susceptibility Tests. J Clin Microbiol. 2023;61(10):e0073923.
37. Callahan BJ, McMurdie PJ, Rosen MJ, Han AW, Johnson AJ, Holmes SP. DADA2: High-resolution sample inference from Illumina amplicon data. Nat Methods. 2016;13:581–3.
38. McDonald D, Jiang Y, Balaban M, et al. Greengenes2 unifies microbial data in a single reference tree. Nat Biotechnol. 2024;42:715–8.
39. Pham TP, Cadoret F, Tidjani Alou M, Brah S, Ali Diallo B, Diallo A, et al. *Marasmitruncus massiliensis*' gen. nov., sp. nov., '*Clostridium culturomicum*' sp. nov., '*Blautia provencensis*' sp. nov., '*Bacillus caccae*' sp. nov. and '*Ornithinibacillus massiliensis*' sp. nov., isolated from stool samples of undernourished African children. New Microbes New Infect. 2017;19:38–42.
40. Shin NR, Whon TW, Kim MS, et al. *Ornithinibacillus scapharcae* sp. nov., isolated from a dead ark clam. Antonie Van Leeuwenhoek. 2012;101(1):147–54.
41. Tan IS, Ramamurthi KS. Spore formation in *Bacillus subtilis*. Environ Microbiol Rep. 2014;6(3):212–25.
42. Zhang J, Fitz-James PC, Aronson AI. Cloning and characterization of a cluster of genes encoding polypeptides present in the insoluble fraction of the spore coat of *Bacillus subtilis*. J Bacteriol. 1993;175(12):3757–66.
43. Scheller D, Becker F, Wimbert A, Meggers D, Pienkoß S, Twittenhoff C, Knoke LR, Leichert LI, Narberhaus F. The oxidative stress response, in particular the katY gene, is temperature-regulated in *Yersinia pseudotuberculosis*. PLoS Genet. 2023;19(7):e1010669.
44. Li W, Gao L, Huang W, Ma Y, Muhammad I, Hanif A, Ding Z, Guo X. Antioxidant properties of lactic acid bacteria isolated from traditional fermented yak milk and their probiotic effects on the oxidative senescence of *Caenorhabditis elegans*. Food Funct. 2022;13(6):3690–703.
45. Hooper DC, Jacoby GA. Mechanisms of drug resistance: quinolone resistance. Ann N Y Acad Sci. 2015;1354(1):12–31.
46. Poirel L, Jayol A, Nordmann P. Polymyxins: antibacterial activity, susceptibility testing, and resistance mechanisms encoded by plasmids or chromosomes. Clin Microbiol Rev. 2017;30(2):557–96.
47. Hof H. An update on the medical management of listeriosis. Expert Opin Pharmacother. 2004;5(8):1727–35.
48. Guillet C, Join-Lambert O, Le Monnier A, et al. Human listeriosis caused by Listeria ivanovii. Emerg Infect Dis. 2010;16(1):136–8.
49. Sauvage E, Kerff F, Terrak M, Ayala JA, Charlier P. The penicillin-binding proteins: structure and role in peptidoglycan biosynthesis. FEMS Microbiol Rev. 2008;32(2):234–58.
50. Perry JA, Wright GD. The antibiotic resistance mobilome: searching for the link between environment and clinic. Front Microbiol. 2013;4:138.
51. Gertz RE Jr, Pimenta FC, Chochua S, Larson S, Venero AK, Bigogo G, Milucky J, Carvalho MDG, Beall B. Nonpneumococcal Strains Recently Recovered from Carriage Specimens and Expressing Capsular Serotypes Highly Related or Identical to Pneumococcal Serotypes 2, 4, 9A, 13, and 23A. mBio. 2021;12(3):e01037–21.
52. Porsch EA, Kehl-Fie TE, St Geme. JW 3rd. Modulation of *Kingella kingae* adherence to human epithelial cells by type IV Pili, capsule, and a novel trimeric autotransporter. mBio. 2012;3(5):e00372–12.
53. Beveridge TJ. Use of the gram stain in microbiology. Biotech Histochem. 2001;76(3):111–8.
54. Sutcliffe IC. A phylum level perspective on bacterial cell envelope architecture. Trends Microbiol. 2010;18(10):464–70.
55. Martínez-Porchas M, Villalpando-Canchola E, Vargas-Albores F. Significant loss of sensitivity and specificity in the taxonomic classification occurs when short 16S rRNA gene sequences are used. Heliyon. 2016;2(9):e00170.
56. Abellan-Schneyder I, Matchado MS, Reitmeier S, Sommer A, Sewald Z, Baumbach J, List M, Neuhaus K. Primer, Pipelines, Parameters: Issues in 16S rRNA Gene Sequencing. mSphere. 2021;6(1):e01202–20.
57. Kuek LE, Lee RJ. First contact: the role of respiratory cilia in host-pathogen interactions in the airways. Am J Physiol Lung Cell Mol Physiol. 2020;319(4):L603–19.

Publisher's Note